

MICROWAVE SPECTRUM AND STRUCTURE OF VANADYL(V) CHLORIDE

Ken-ichi KARAKIDA and Kozo KUCHITSU

Department of Chemistry, Faculty of Science

The University of Tokyo, Bunkyo-ku, Tokyo 113, Japan

and

Chi MATSUMURA

Government Chemical Industrial Research Institute, Tokyo

Shibuya-ku, Tokyo 151, Japan

The microwave spectrum of vanadyl(V) chloride was measured, and the following rotational constants (in MHz) were determined: $B_O = 1741.72 \pm 0.01$ for $OV^{35}Cl_3$, $B_O = 1665.20 \pm 0.02$ for $OV^{37}Cl_3$, $A_O = 1739.94 \pm 0.05$, $B_O = 1692.17 \pm 0.05$, $C_O = 1139 \pm 1$ for $OV^{35}Cl_2^{37}Cl$. From these constants the r_O structure was determined: $r(V-O) = 1.595 \pm 0.005$ Å, $r(V-Cl) = 2.131 \pm 0.001$ Å and $\angle(Cl-V-Cl) = 111.8 \pm 0.2^\circ$.

In a number of recent studies, precise structures of PX_3 and YPX_3 molecules ($Y=O, S; X=F, Cl, Br$) have been determined by means of gas electron diffraction and microwave spectroscopy.¹⁻³ As an extension of these studies, our attention has been drawn to a vanadium compound, $OVCl_3$. The only existing literature on the structure of $OVCl_3$ is that of Palmer,⁴ who made a visual electron-diffraction study. Accordingly, the present study has been undertaken to determine a more precise structure by means of microwave spectroscopy.

Analysis of Microwave Spectrum

A sample of $OVCl_3$ (purity over 99 %, bp $149-151^\circ C/176$ Torr) obtained from a commercial source was used without further purification. A conventional spectrometer with 100 KHz square-wave Stark modulation was used at room temperature. As the sample was found to decompose rapidly in the cell, it was continuously introduced into the cell and pumped out during the measurement.

The rotational lines of $^{16}O^{51}V^{35}Cl_3$, $^{16}O^{51}V^{37}Cl_3$ and $^{16}O^{51}V^{35}Cl_2^{37}Cl$ were assigned (Tables 1-3). The absorption lines corresponding to $J \lesssim 7$ have half-width of 1-2 MHz and are nearly symmetric with unresolved hyperfine structures due to the nuclear quadrupole coupling of ^{35}Cl , ^{37}Cl ($I=3/2$) and ^{51}V ($I=7/2$). The transition frequencies were measured from the peak positions. No detailed analysis of this coupling was made. For transitions corresponding to $J \gtrsim 10$, on the other hand, the line shapes are essentially determined by the centrifugal distortion constant D_{JK} , and the effect of quadrupole coupling is relatively unimportant.

The spectroscopic constants obtained are given in Table 4. The centrifugal distortion constants D_J for $OV^{37}Cl_3$ and $OV^{35}Cl_2^{37}Cl$ were calculated from those for $OV^{35}Cl_3$ on the assumption that D_J is proportional to B_O^4/C_O and $[1/2(A_O + B_O)]^4/C_O$, respectively.⁵ (C_O was estimated from the r_O structure determined in this study.) The D_{JK} for $OV^{35}Cl_3$ was determined by an envelope analysis of the unresolved K components for $J=10-18$. This calculation was based on a

Table 1. Transition frequencies of $\text{OV}^{35}\text{Cl}_3$ (MHz)

	Obsd.	Calcd.	O-C
J= 5 \leftarrow 4	17417.04	17416.94	0.10
6 \leftarrow 5	20900.16	20900.18	-0.02
7 \leftarrow 6	24383.34	24383.36	-0.02
8 \leftarrow 7	27866.44	27866.44	0.00
9 \leftarrow 8	31349.46	31349.49	-0.03
10 \leftarrow 9	34832.42	34832.39	0.03
11 \leftarrow 10	38315.14	38315.16	-0.02
12 \leftarrow 11	41797.77	41797.78	-0.01
13 \leftarrow 12	45280.15	45280.23	-0.08
14 \leftarrow 13	48762.60	48762.52	0.08
15 \leftarrow 14	52244.61	52244.63	-0.02
16 \leftarrow 15	55726.64	55726.55	0.09

Table 2. Transition Frequencies of $\text{OV}^{37}\text{Cl}_3$ (MHz)

	Obsd.	Calcd.	O-C
J=13 \leftarrow 12	43291.20	43291.28	-0.08
14 \leftarrow 13	46620.90	46620.67	0.23
15 \leftarrow 14	49949.88	49949.91	-0.03
16 \leftarrow 15	53278.94	53278.98	-0.04
17 \leftarrow 16	56607.74	56607.88	-0.14

Table 3. Transition Frequencies of $\text{OV}^{35}\text{Cl}_2^{37}\text{Cl}$ (MHz)

	Obsd.	Calcd.	O-C
10 ₉ 2 \leftarrow 9 ₈ 2	34391.72	34391.70	0.02
10 ₈ 2 \leftarrow 9 ₇ 2	34104.68	34104.62	0.06
10 ₈ 3 \leftarrow 9 ₇ 3	34290.15	34290.17	-0.02
10 ₇ 3 \leftarrow 9 ₆ 3	34212.19	34212.11	0.08
10 ₇ 4 \leftarrow 9 ₆ 4	34284.15	34284.08	0.07
10 ₆ 4 \leftarrow 9 ₅ 4	34278.03	34277.98	0.05
11 ₉ 2 \leftarrow 10 ₈ 2	37514.16	37514.09	0.07
11 ₉ 3 \leftarrow 10 ₈ 3	37721.18	37721.17	0.01
11 ₈ 3 \leftarrow 10 ₇ 3	37603.95	37603.83	0.12
11 ₈ 4 \leftarrow 10 ₇ 4	37706.47	37706.58	-0.11
11 ₇ 4 \leftarrow 10 ₆ 4	37694.71	37694.64	0.07
12 ₁₁ 2 \leftarrow 11 ₁₀ 2	41306.66	41306.64	0.02
12 ₁₀ 2 \leftarrow 11 ₉ 2	40932.18	40932.21	-0.03
12 ₁₀ 3 \leftarrow 11 ₉ 3	41154.87	41154.82	0.05
12 ₉ 3 \leftarrow 11 ₈ 3	40989.88	40989.98	-0.10
12 ₉ 4 \leftarrow 11 ₈ 4	41128.22	41128.38	-0.16
12 ₈ 4 \leftarrow 11 ₇ 4	41106.76	41106.64	0.12
14 ₁₂ 3 \leftarrow 13 ₁₁ 3	48032.31	48032.28	0.03
14 ₁₁ 3 \leftarrow 13 ₁₀ 3	47759.18	47759.13	0.05
14 ₁₁ 4 \leftarrow 13 ₁₀ 4	47971.97	47971.94	0.03
14 ₁₀ 5 \leftarrow 13 ₉ 5	47982.38	47982.58	-0.20
14 ₉ 5 \leftarrow 13 ₈ 5	47977.83	47977.68	0.15
14 ₉ 6 \leftarrow 13 ₈ 6	47999.14	47999.13	0.01

simulation of each spectral contour of a given J from its K components of the Lorentz shape with an assumed half-width of 0.4 MHz. Typical observed and best-fit envelopes are illustrated in Fig. 1. The transition frequencies calculated from these spectroscopic constants are compared with the corresponding observed frequencies in Tables 1-3. This envelope analysis showed slight shifts of the peak positions (less than 0.2 MHz) due to D_{JK} from their hypothetical unsplit values. The calculated frequencies in Table 1 include corrections for these shifts. The corresponding shifts for $\text{OV}^{37}\text{Cl}_3$ were estimated to be essentially equal from the assumption that isotopic D_{JK} is roughly proportional to $^{5}\text{B}_\text{O}^4/\text{C}_\text{O}$. The D_{JK} for $\text{OV}^{35}\text{Cl}_2^{37}\text{Cl}$, derived from the analysis with symmetric-top approximation, was consistent with the value obtained from the envelope analysis of the $\text{OV}^{35}\text{Cl}_3$ spectrum.

Table 4. Spectroscopic Constants (MHz)

$\text{OV}^{35}\text{Cl}_3$	$B_0 = 1741.72 \pm 0.01$	$\text{OV}^{35}\text{Cl}_2^{37}\text{Cl}$	$A_0 = 1739.94 \pm 0.05$
	$D_J = (0.53 \pm 0.02) \times 10^{-3}$		$B_0 = 1692.17 \pm 0.05$
	$D_{JK} = -(0.9 \pm 0.2) \times 10^{-3}$		$C_0 = 1139 \pm 1$
$\text{OV}^{37}\text{Cl}_3$	$B_0 = 1665.20 \pm 0.02$		$D_{JK} = -(0.9 \pm 0.2) \times 10^{-3}$

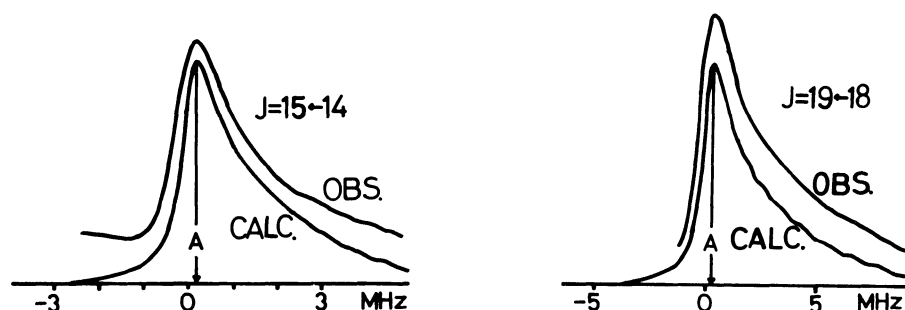


Fig. 1. Typical observed and calculated envelopes for $\text{OV}^{35}\text{Cl}_3$ ($D_{JK} = -0.9 \times 10^{-3}$ MHz). Slight shifts in the peak positions (A) due to D_{JK} from their hypothetical unsplit values (the origin of the abscissa) are observed.

Errors in Structural Parameters

The r_0 structure of OVCl_3 , which satisfies the five rotational constants listed in Table 4, is given in Table 5. The uncertainties in the three parameters were estimated by taking differences between the observed rotational constants and those calculated with varying parameter values; no set of the parameters outside the quoted error limits can reproduce all the observed rotational constants within their experimental errors.

This situation may be displayed in a three-dimensional diagram. The most-probable set corresponds to a point P, where five surfaces representing the rotational constants meet one another. A cross section of this parameter space, perpendicular to the $r(\text{V-O})$ parameter axis and including P, is shown in Fig. 2. A pair of broken lines, which run parallel to a solid line C, correspond to the estimated limit of error of the rotational constant C_0 for $\text{OV}^{35}\text{Cl}_2^{37}\text{Cl}$. The uncertainties in the rest of the rotational constants are much smaller and not displayed in the figure, but they cause appreciable errors in the r_0 parameters because these lines are very nearly parallel to one another. On the other hand, the line C serves to decrease the error limits of the r_0 parameters, since it intersects the rest of the lines with larger angles. The parameter sets which satisfy all the rotational constants forms a region with upper and lower bounds denoted as Q_1 (1.600, 2.130 Å and 111.9° for $r(\text{V-O})$, $r(\text{V-Cl})$ and $\angle\text{Cl-V-Cl}$, respectively) and Q_2 (1.590, 2.132 Å and 111.6°). A projection of this region onto the figure plane specifies the error limits of the $r(\text{V-Cl})$ and $\angle\text{Cl-V-Cl}$ parameters. The error limits of the $r(\text{V-O})$ parameter may be displayed by an alternative projection. It should be noted that the present r_0 structure has been derived directly from the rotational constants for the ground vibrational state without correction for vibration-

Table 5. Structural Parameters of OVCl_3

	$r(\text{V-O}) \text{ \AA}$	$r(\text{V-Cl}) \text{ \AA}$	$\angle \text{Cl-V-Cl}$
Palmer ^a	1.56 ± 0.04	2.12 ± 0.03	$111.2 \pm 2^\circ$
This study ^b	1.595 ± 0.005	2.131 ± 0.001	$111.8 \pm 0.2^\circ$

a) Ref. 4 b) r_0 structure. Systematic errors due to vibrational effects are not included in the quoted uncertainties.

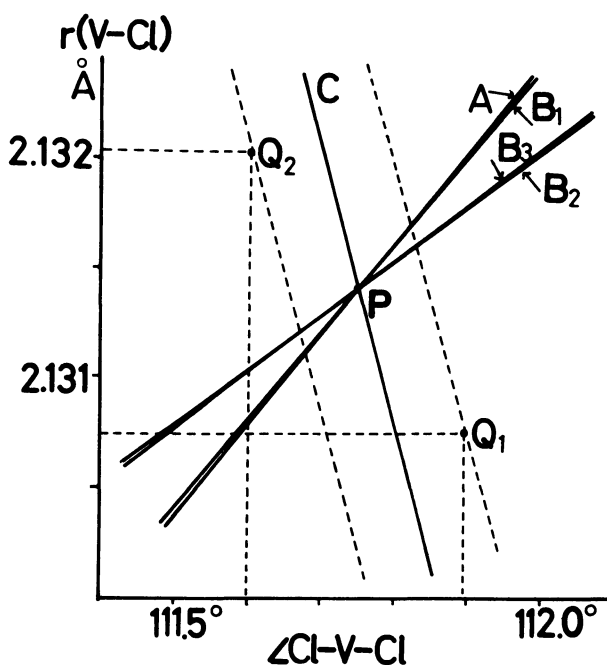


Fig. 2. Two-dimensional parameter space for $r(\text{V-O}) = 1.595 \text{ \AA}$. The set of the parameters which reproduces the observed rotational constants is shown by P. The observed rotational constants correspond to nearly straight lines: B_1 for $\text{OV}^{35}\text{Cl}_3$, B_2 for $\text{OV}^{37}\text{Cl}_3$, and A, B_3 , C for $\text{OV}^{35}\text{Cl}_2^{37}\text{Cl}$. The plane C is very nearly parallel to the $r(\text{V-O})$ axis. A pair of broken lines indicate the uncertainty in C_0 . The upper and lower bounds of the acceptable parameter sets, which are compatible with the observed rotational constants within experimental errors, are denoted as Q_1 (for $r(\text{V-O}) = 1.600 \text{ \AA}$) and Q_2 (for $r(\text{V-O}) = 1.590 \text{ \AA}$). They are projected onto this plane to show the limits of the $r(\text{V-Cl})$ and $\angle \text{Cl-V-Cl}$ parameters.

rotation interaction.

The earlier structure reported by Palmer,⁴ also listed in Table 5, is consistent with the present structure within his experimental error. The vanadium-chlorine bond length, $r_0(\text{V-Cl})$, determined in the present study is nearly equal to the $r_g(\text{V-Cl})$ in VCl_4 determined by gas electron diffraction,⁶ $2.138 \pm 0.002 \text{ \AA}$. The vanadium valence angle ($\angle \text{Cl-V-Cl}$) is about 8° larger than the phosphine valence angle in OPCl_3 ,² $\angle \text{Cl-P-Cl} = 103.3 \pm 0.2^\circ$. An attempt is being made to determine the r_g parameters of this molecule by gas electron diffraction.

References

1. Y. Morino, K. Kuchitsu and T. Moritani, *Inorg. Chem.*, **8**, 867 (1969).
2. T. Moritani, K. Kuchitsu and Y. Morino, *ibid.*, **10**, 344 (1971).
3. K. Kuchitsu, T. Shibata, A. Yokozeki and C. Matsumura, *ibid.*, **10**, 2584 (1971).
4. K.J. Palmer, *J. Amer. Chem. Soc.*, **60**, 2360 (1938).
5. W.H. Shaffer, *J. Chem. Phys.*, **10**, 1 (1942).
6. Y. Morino and H. Uehara, *J. Chem. Phys.*, **45**, 4543 (1966).

(Received February 17, 1972)